Dual Mechanisms of Allosteric Acceleration of the Na^+,K^+-ATPase by ATP

Mohammed Khalid,[†] Flemming Cornelius,[‡] and Ronald J. Clarke[‡*]
[†]School of Chemistry, University of Sydney, Sydney, Australia; and [‡]Department of Physiology and Biophysics, University of Aarhus, Aarhus C, Denmark

ABSTRACT Investigations of the E2 → E1 conformational change of Na^+,K^+-ATPase from shark rectal gland and pig kidney via the stopped-flow technique have revealed major differences in the kinetics and mechanisms of the two enzymes. Mammalian kidney Na^+,K^+-ATPase appears to exist in a diprotomeric $(\alpha\beta)_2$ state in the absence of ATP, with protein-protein interactions between the α-subunits causing an inhibition of the transition, which occurs as a two-step process: E2:E2 → E2:E1 → E1:E1. This is evidenced by a biphasicity in the observed kinetics. Binding of ATP to the E1 or E2 states causes the kinetics to become monophasic and accelerate, which can be explained by an ATP-induced dissociation of the diprotomer into separate $\alpha\beta$ protomers and relief of the preexisting inhibition. In the case of enzyme from shark rectal gland, the observed kinetics are monophasic at all ATP concentrations, indicating a monoprotomeric enzyme; however, an acceleration of the E2 → E1 transition by ATP still occurs, to a maximum rate constant of 182 (± 6) s^{-1}. This indicates that ATP has two separate mechanisms whereby it accelerates the E2 → E1 transition of Na^+,K^+-ATPase $\alpha\beta$ protomers and $(\alpha\beta)_2$ diprotomers.

INTRODUCTION

The most widely used model of the mechanism of P-type ATPases is the Albers-Post or E1-E2 model (1,2). In the case of the Na^+,K^+-ATPase, the E2 → E1 transition of the unphosphorylated enzyme and its associated release of K^+ ions to the cytoplasm are dramatically accelerated by the presence of ATP (3). This acceleration is crucial to the enzyme under physiological conditions, because the E2 → E1 transition is one of the rate-determining steps of the enzyme's reaction cycle (4–6). Therefore, ATP plays a critical role in modulating the rate of ion pumping as well as providing the necessary energy.

However, the mechanism by which ATP accelerates the E2 → E1 transition of the Na^+,K^+-ATPase is still uncertain. A fundamental question is whether the acceleration is evident in the case of a single Na^+,K^+-ATPase protomer, consisting of the catalytic α-subunit and the smaller β-subunit, or whether the acceleration requires the enzyme to exist in a diprotomeric $(\alpha\beta)_2$ or higher oligomeric state. We recently suggested (1) a mechanism based on recent crystal structures of the related enzyme, the sarcoplasmic reticulum Ca^{2+}-ATPase (7,8), whereby ATP binding to an $(\alpha\beta)_2$ diprotomer causes the cytoplasmic domains of its α-subunits to take up a more compact conformation, thus lessening the degree of contact between neighboring α-subunits within the membrane and allowing each of them to undergo the transition to the E1 state at a faster rate. In this mechanism, the acceleration of the E2 → E1 transition can be attributed to an ATP-induced relief of a preexisting steric inhibition due to contacts between the α-subunits within an $(\alpha\beta)_2$ diprotomer. Therefore, such a mechanism could only operate if, before ATP binding occurs, the enzyme exists in a diprotomeric or oligomeric state. However, Ward and Cavieres (9) reported that, even in the case of enzyme solubilized as $\alpha\beta$ protomers using the detergent $C_{12}E_8$, a low-affinity ATP acceleration of the enzyme's activity exists. Therefore, it seems possible that there may be two separate allosteric effects of ATP—one acting on $\alpha\beta$ protomers, and the other on $(\alpha\beta)_2$ diprotomers. That is the hypothesis under investigation in this paper.

In an earlier study (10), we demonstrated the involvement of an $(\alpha\beta)_2$ diprotomer in the E2 → E1 conformational kinetics by studying its ATP concentration dependence using the voltage-sensitive probe RH421. At zero or low ATP concentrations (<50 μM), biphasic kinetics were observed. This was attributed to a two-step process within an $(\alpha\beta)_2$ diprotomer, i.e., E2:E2 → E2:E1 → E1:E1. At higher ATP concentrations, the kinetics became monophasic. This could be accounted for by ATP binding causing the cytoplasmic domains to close together, thus dissociating the diprotomers into separate protomers. The observation of biphasic kinetics of the E2 → E1 transition at low concentrations of ATP can, therefore, be taken as an indication of rate determination of the transition via protein-protein interactions within an $(\alpha\beta)_2$ diprotomer. It is important to note, however, that the measurements that led to the postulation of the diprotomeric mechanism of ATP-induced acceleration of the E2 → E1 transition were carried out on Na^+,K^+-ATPase purified from rabbit kidney.

In the case of enzyme purified from mammalian kidney preparations, the maximum rate constant for the E2 → E1 transition appears to be in the range of 30–90 s^{-1} (3,5,10–12) at saturating ATP concentrations at 24°C and pH 7.4. At the lower temperature of 20°C, however, Cornelius et al. (13) found that enzyme isolated from shark rectal gland already had a rate constant of >80 s^{-1}. In an earlier study

Submitted December 13, 2009, and accepted for publication January 20, 2010.

*Correspondence: r.clarke@chem.usyd.edu.au

Editor: Patrick Loria.

0006-3495/10/05/2290/9 $2.00

doi: 10.1016/j.bpj.2010.01.038

by Lüpfert et al. (3), the rate constant for the E2 → E1 transition of shark enzyme was determined to be ~132 s^{-1} at 24°C, whereas the turnover number of the same enzyme was calculated to be 70 s^{-1} at the same temperature. Lüpfert et al. (3) also determined the turnover numbers of pig and rabbit kidney enzyme preparations to be 48 and 43 s^{-1}, respectively. A comparison of the turnover numbers and rate constants determined for the E2 → E1 transition for these preparations shows that whereas the E2 → E1 transition is the major rate-determining step for the mammalian kidney enzymes at saturating ATP concentrations, this is not the case for the shark enzyme. To account for its turnover number of 70 s^{-1} at 24°C, there must be another, slower reaction in the shark enzyme's reaction cycle. Based on quenched-flow (13,14) studies, this reaction appears to be the K^+-stimulated dephosphorylation.

To understand the more-rapid kinetics for the E2 → E1 transition of the shark enzyme relative to the mammalian kidney enzymes, we decided to carry out a more detailed comparison of the shark rectal gland and pig kidney enzymes. Cornelius et al. (13) and Lüpfert et al. (3) investigated the kinetics of the E2 → E1 transition by coupling it to the subsequent phosphorylation reaction by ATP and following the kinetics of the buildup in the E2P state using the voltage-sensitive probe RH421. This has the advantage of increasing the amplitude of the observed fluorescence change, but it complicates the interpretation of the kinetics because a series of reactions are involved. In this study, we investigated the E2 → E1 transition in more detail by isolating it from any other reactions. This enabled us to suggest that, in contrast to kidney, the shark enzyme behaves kinetically purely as an $\alpha\beta$ protomer, and that ATP induces accelerations in the E2 → E1 transition of both protomeric and diprotomeric enzymes but via different mechanisms.

MATERIALS AND METHODS

Enzyme and reagents

Na^+,K^+-ATPase-containing membrane fragments from shark rectal gland and pig kidney were purified as described by Skou and Esmann (15) and Klodos et al. (16), respectively. The specific ATPase activities at 37°C and pH 7.4 were measured according to Ottolenghi (17). The activities of the preparation used were 1765 and 1365 μmol ATP hydrolyzed h^{-1} (mg of protein)$^{-1}$ at saturating substrate concentrations for shark and pig enzyme, respectively. The protein concentrations were 6.8 mg mL^{-1} and 4.7 mg mL^{-1} for shark and pig enzyme, respectively. The concentrations were determined according to the Peterson modification (18) of the Lowry method (19) using bovine serum albumin as a standard. To calculate the molar protein concentration, a molecular mass for an $\alpha\beta$ unit of the Na^+,K^+-ATPase of 147,000 g mol^{-1} (20) was used.

N-(4-Sulfobutyl)-4-(4-(*p*-(dipentylamino)phenyl)butadienyl)-pyridinium salt (RH421) was obtained from Molecular Probes (Eugene, OR) and used without further purification. RH421 was added to Na^+,K^+-ATPase-containing membrane fragments from an ethanolic stock solution. The dye spontaneously partitioned into the membrane fragments.

The following reagents were used: L-histidine (≥99.5%; Fluka, Castle Hill, Australia), imidazole (≥99%; Sigma, Castle Hill, Australia), NaCl (suprapure grade; Merck, Kilsyth, Australia), $MgCl_2 \cdot 6H_2O$ (analytical grade; Merck), EDTA (99%, Sigma), ATP disodium$\cdot 3H_2O$ (special quality; Roche, Castle Hill, Australia), NaOH (analytical grade; Merck), and HCl (0.1 N Titrisol solution; Merck).

Stopped-flow spectrofluorimetry

Stopped-flow experiments were carried out using an SF-61 stopped-flow spectrofluorimeter from Hi-Tech Scientific (Salisbury, UK) as described previously (10). Briefly, the kinetics of conformational changes of unphosphorylated enzyme were investigated in the stopped-flow apparatus by mixing Na^+,K^+-ATPase labeled with RH421 with an equal volume of 130 mM NaCl alone or containing varying concentrations of Na_2ATP. Both the enzyme suspension and the NaCl/Na_2ATP mixtures were prepared in a solution containing 25 mM histidine and 0.1 mM EDTA. The pH of the solution was adjusted to 7.4 with HCl. It should be noted that at this pH value, histidine no longer functions well as a buffer. Nevertheless, its use in combination with EDTA allows the pH to be adjusted to pH 7.4 and prevents the introduction to the medium of buffer cations, which are known to bind to the enzyme in a fashion similar to Na^+ ions and stabilize an E1-like conformation (3,21–28). The conformational equilibrium of the enzyme was thus initially poised toward the E2 conformation. Experiments were also performed in a solution containing 1 mM KCl in addition to 25 mM histidine and 0.1 mM EDTA to initially stabilize the E2$(K^+)_2$ state of the enzyme.

In another experiment to determine the kinetics of the E2 → E1 transition, enzyme labeled with RH421 was equilibrated in a solution containing 25 mM histidine and 0.1 mM EDTA, and then rapidly mixed in the stopped-flow apparatus with a phosphorylating solution containing 5 mM $MgCl_2$, 130 mM NaCl, 2 mM Na_2ATP, 25 mM histidine, and 0.1 mM EDTA. In this type of experiment, the enzyme undergoes the reaction sequence E2 → E1$(Na^+)_3$ → E1P$(Na^+)_3$ → E2P + $3Na^+$. However, since the rate-determining step in this sequence at saturating ATP concentrations is the E2 → E1 transition, this experiment also gives a good estimate of the rate constant of the transition (3,13).

To improve the signal/noise ratio, typically 11–23 experimental traces were averaged before the observed rate constants, k_{obs}, and the fluorescence amplitudes, $\Delta F/F_0$, were evaluated. This was done by fitting either one or a sum of two exponential functions to the averaged experimental trace. The choice between a single or double exponential fit was made on the basis of the presence or absence of any observed deviation from random fluctuation in residual plots and the values of the χ^2 parameter. If no obvious deviation from random fluctuation of the residual plots was observable, the single exponential fit was preferred.

Simulations

Computer simulations of the time course of fluorescence changes observed experimentally via stopped-flow spectrofluorimetry were performed using the commercially available program Berkeley Madonna 8.0 and the variable step-size Rosenbrock integration method for stiff systems of differential equations. The simulations yielded the time course of the concentration of each enzyme intermediate involved, as well as the total fluorescence. For the purposes of the simulations, each enzyme intermediate was normalized to a unitary enzyme concentration.

RESULTS

Kinetics of the E2 → E1 transition in the absence of ATP

Previously performed stopped-flow investigations (10) on enzyme purified from rabbit kidney have shown that in the complete absence of ATP or at low ATP concentrations (<50 μM), the kinetics of the E2 → E1 transition follow a

biphasic time course. As stated in the Introduction, this can be explained by a two-step reaction: E2:E2 → E2:E1(Na^+)$_3$ → E1(Na^+)$_3$:E1(Na^+)$_3$. A dimeric mechanism is required to explain the data because the probe used to follow the kinetics, RH421, is known to respond in rabbit enzyme only to the electrogenic binding of the third Na^+ ion to the E1 state (29,30). Since it is already well established that each α-subunit possesses only three Na^+ transport sites, a two-step binding of three Na^+ ions necessarily requires a dimer.

We then sought to determine whether biphasic kinetics is a general characteristic of the E2 → E1 transition at zero or low ATP concentrations for the Na^+,K^+-ATPase from all sources. Based on the results shown in Fig. 1, the answer is clearly no. Whereas the transients obtained with pig kidney enzyme (Fig. 1 *B*) were clearly biphasic, as previously observed for rabbit kidney enzyme (10), for the shark rectal gland enzyme there was no necessity to include a second exponential to adequately fit the data. The shark enzyme transients appeared to be purely monophasic (Fig. 1 *A*).

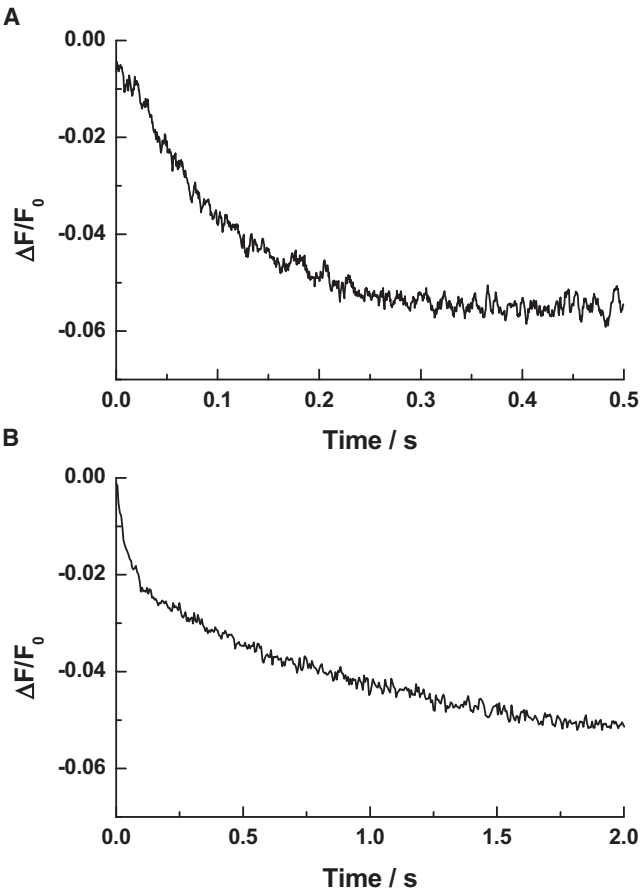

FIGURE 1 Stopped-flow fluorescence transients of Na^+,K^+-ATPase from (*A*) shark rectal gland and (*B*) pig kidney noncovalently labeled with RH421 (500 nM, after mixing). Na^+,K^+-ATPase (40 μg/mL or 0.27 μM, after mixing) was rapidly mixed with an equal volume of a solution containing 130 mM NaCl (pH 7.4, 24°C). Both the enzyme suspensions and the NaCl solution were prepared in a solution containing 25 mM histidine and 0.1 mM EDTA. The fluorescence of membrane-bound RH421 was measured at an excitation wavelength of 577 nm at emission wavelengths of ≥665 nm (RG665 glass cutoff filter). The calculated observed rate constants were (*A*) 10.6 (± 0.3) s^{-1} for the shark enzyme and (*B*) 25 (± 3) s^{-1} (35% of the total amplitude) and 0.94 (± 0.02) s^{-1} (65%) for the pig enzyme.

To test the appropriateness of the double exponential fit of the pig enzyme data shown Fig. 1 *B*, we carried out a statistical *F*-test. The curve shown is an average of 14 individual traces, each consisting of 1024 data points (n). The χ^2 parameters derived from the commercial software supplied with the stopped-flow fluorimeter for single exponential (two fitting parameters, p_1) and double exponential (four fitting parameters, p_2) fits to the data were 3.23 and 1.2, respectively. Calculating F according to the equation $[(\chi_1^2 - \chi_2^2)/(p_2 - p_1)]/[\chi_2^2/(n - p_2)]$ yields a value of 863. For this combination of fitting parameter values for each fitting function, this F value is significantly greater than the critical value of 18 for a 1% probability of the null hypothesis that the double exponential fit is no better than the single exponential fit for these data. Based on this quantitative assessment, we conclude that the biphasic behavior of the pig kidney enzyme is statistically significant.

ATP concentration dependence of the kinetics of the E2 → E1 transition

To measure the ATP concentration dependence of the kinetics of the E2 → E1 transition, we measured both the shark and the pig enzymes in the stopped-flow apparatus by rapidly mixing them with 25 mM histidine solution containing 130 mM NaCl and varying concentrations of Na_2ATP, as described in Materials and Methods. In the case of the shark enzyme, the observed transients were always monophasic, regardless of the ATP concentration (see Figs. 1 and 2). The magnitude of the fluorescence change, $\Delta F/F_0$, was ~−0.056 in the absence of ATP and then always in the range of −0.062 to −0.085 for all ATP concentrations. The observed rate constants, k_{obs}, as a function of the ATP concentration, determined from monoexponential fits to the experimental data, are shown in Fig. 3. It can be seen that k_{obs} increases hyperbolically to a maximum value of 182 (± 6) s^{-1}. To obtain an estimate for the low-affinity dissociation constant of ATP with the E2 state, K_d, the following equation was fitted to the data:

$$k_{obs} = k_{obs}^{min} + \left(k_{obs}^{max} - k_{obs}^{min}\right) \cdot \frac{[ATP]}{K_d + [ATP]} \qquad (1)$$

where k_{obs}^{min} and k_{obs}^{max} are the values of k_{obs} at infinitely low and infinitely high concentrations of ATP, respectively. The value of K_d obtained from the fit was 63 (± 12) μM. This value is similar in magnitude to the value previously reported (10,12) for rabbit kidney enzyme of 71 (± 7) μM from the same type of measurement under the same conditions. However, the value of k_{obs}^{max} of 182 (± 6) s^{-1} is significantly higher than the value determined for rabbit,

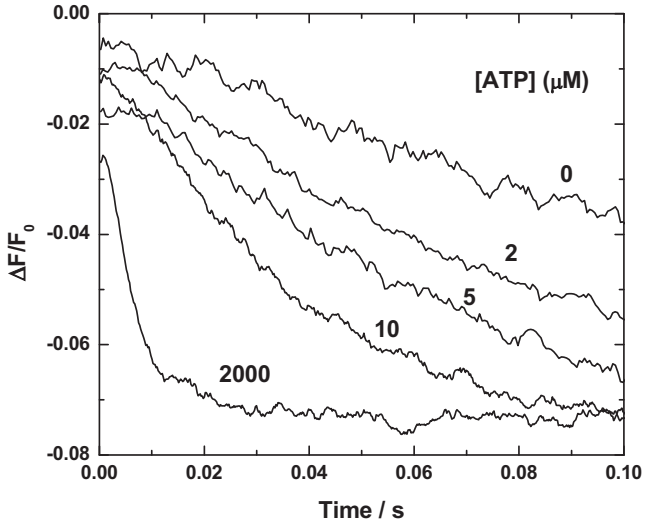

FIGURE 2 Stopped-flow fluorescence transients of the E2 → E1 transition of Na^+,K^+-ATPase from shark rectal gland nonovalently labeled with RH421. The transition was induced by rapid mixing with 130 mM NaCl and varying concentrations of Na_2ATP. All experimental conditions were as described in Fig. 1. The labels 0, 2, 5, 10, and 2000 represent the ATP concentration after mixing in μM. The calculated observed rate constants were 0 ATP, 10.6 (± 0.3) s^{-1}; 2 μM ATP, 17 (± 1) s^{-1}; 5 μM ATP, 23 (± 3) s^{-1}; 10 μM ATP, 32 (± 2) s^{-1}; and 2000 μM ATP 166 (± 4) s^{-1}.

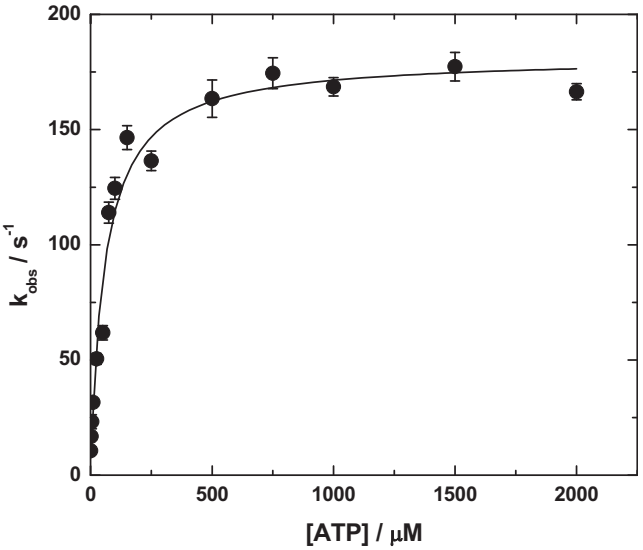

FIGURE 3 Dependence of the observed rate constant of the RH421 fluorescence change on the concentration of Na_2ATP (after mixing) for stopped-flow experiments in which Na^+,K^+-ATPase from shark rectal gland in a solution containing 25 mM histidine and 0.1 mM EDTA was rapidly mixed with the same histidine/EDTA solution containing 130 mM NaCl and varying concentrations of Na_2ATP. [Na^+,K^+-ATPase] = 40 μg/mL (0.27 μM), [RH421] = 500 nM; pH = 7.4, T = 24°C. The solid line is a nonlinear least-squares fit of the data to Eq. 1. The fit parameters were k_{obs}^{min} = 9 (± 6) s^{-1}; k_{obs}^{max} = 182 (± 6) s^{-1}; and K_d = 63 (± 12) μM.

which was only 39 (± 1) s^{-1} (11). The value of k_{obs}^{max} determined here is consistent with measurements of the rate of the E2 → E1 transition at saturating ATP concentrations obtained by a different experimental procedure (3,13). Nevertheless, as a check of the value, we also determined the rate constant of the E2 → E1 transition by preequilibrating the enzyme in 25 mM histidine solution to stabilize the E2 state, and mixing it with a phosphorylating solution containing Mg^{2+} in addition to Na^+ and ATP (see Materials and Methods for details). At an ATP concentration of 1 mM after mixing, the k_{obs} value obtained was 152 (± 5) s^{-1}, which is consistent with the data shown in Fig. 3. Therefore, the rate constant for the E2 → E1 transition at saturating ATP concentrations for the shark enzyme appears to be almost fivefold faster than that of rabbit kidney enzyme under the same conditions.

When the kinetics of the E2 → E1 transition of the pig kidney enzyme were investigated as a function of the ATP concentration, it was found that the biphasic behavior observed in the absence of ATP disappeared at ATP concentrations ≥ 50 μM (see Fig. 4), and thus the observed transients could be fitted perfectly well to a monoexponential time function (as indicated by the lack of any systematic deviations in the residuals plot). At 0.5 μM ATP the biphasic behavior is still obvious by eye, at 2 μM ATP the biphasic behavior is becoming less prominent, and at 150 and 1500 μM ATP there is no evidence of any biphasic behavior at all. This behavior is in complete agreement with previously reported data obtained using rabbit kidney enzyme (10), but is in contrast to the shark enzyme data described above, which showed monophasic kinetics at all ATP concentrations.

For the pig kidney enzyme, there was an increase in the absolute total amplitude, $\Delta F/F_0$, of the observed transients from ~−0.057 in the absence of ATP to ~−0.11 at 2000 μM ATP (see Fig. 5). Because of the more-complex kinetics observed in the case of pig enzyme, it is not possible to simply derive a dissociation constant from the ATP concentration dependence of the observed rate constants. An adequate explanation of the observed behavior requires a combination of information derived from both the kinetics and the amplitudes. The fact that the amplitude of the fluorescence change increases with increasing ATP concentration indicates that the E2 → E1 is reversible, since an irreversible reaction would go to completion regardless of the ATP concentration, yielding a constant ATP-concentration-independent amplitude. A mechanism that can explain the increase in amplitude, the acceleration of the kinetics, and the disappearance of biexponential behavior with increased ATP concentration is shown in Fig. 6. We developed this mechanism in a previous study to explain similar behavior observed for rabbit kidney enzyme (10). In that work, we considered possible alternative explanations for the biphasicity at low ATP concentrations, i.e., the presence of enzyme in a mixture of states between E1 and E2 prior to mixing with NaCl, and the presence of enzyme heterogeneity due to different isoforms, different complexes with FXYD proteins, or different modifications of the protein via the detergent

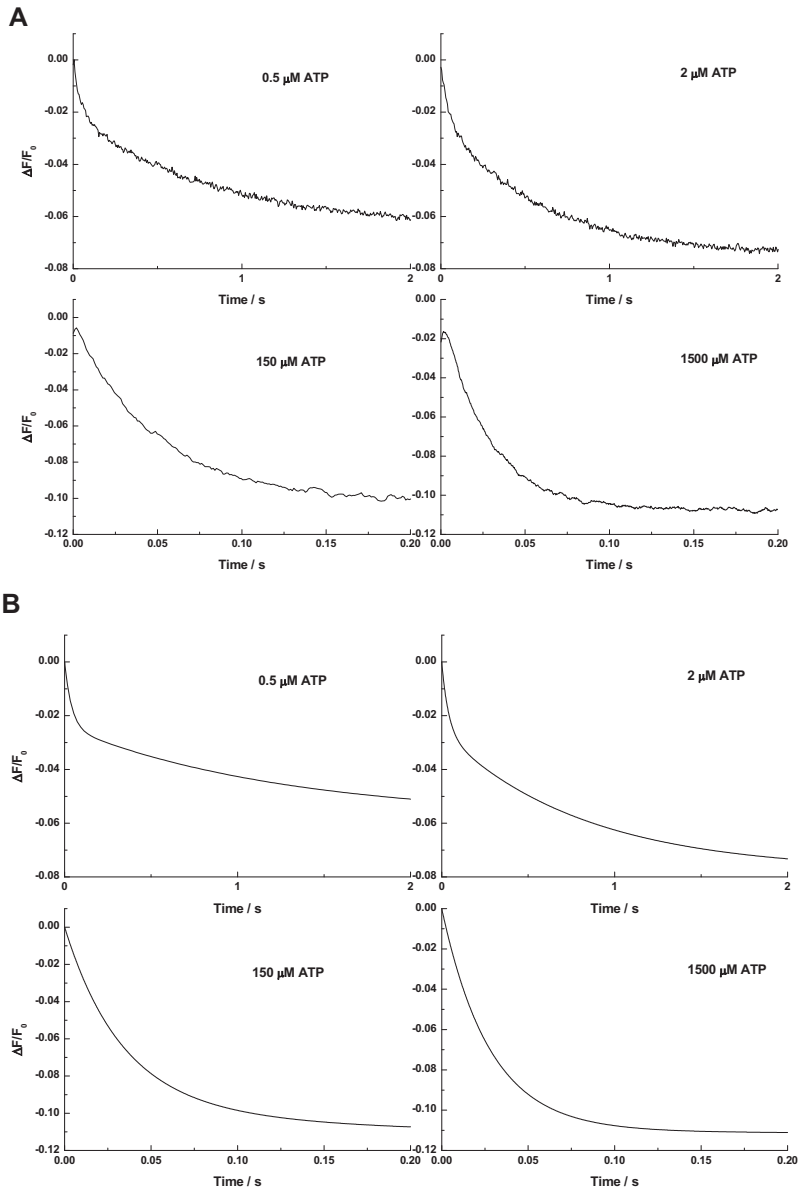

FIGURE 4 (*A*) Stopped-flow fluorescence transients of Na^+,K^+-ATPase from pig kidney noncovalently labeled with RH421 (500 nM, after mixing). Na^+,K^+-ATPase (40 μg/mL or 0.27 μM, after mixing) was rapidly mixed with an equal volume of a solution containing 130 mM NaCl and varying concentrations of Na_2ATP (pH 7.4, 24°C). Both the enzyme suspension and the NaCl/Na_2ATP solution were prepared in a solution containing 25 mM histidine and 0.1 mM EDTA. Excitation and emission wavelengths were as described in the caption to Fig. 3. The calculated observed rate constants were (*a*) 0.5 μM ATP, 24 ($\pm$ 3) s^{-1} (31% of the total amplitude) and 1.32 ($\pm$ 0.02) s^{-1} (69%); (*b*) 2 μM ATP, 27 ($\pm$ 4) s^{-1} (27%) and 1.86 ($\pm$ 0.03) s^{-1} (73%); (*c*) 150 μM ATP 20.4 ($\pm$ 0.2) s^{-1}; and (*d*) 1500 μM ATP 36.3 ($\pm$ 0.2) s^{-1}. (*B*) Kinetic simulations of the experimental fluorescence transients based on a reversible dimeric conformational change model (see Fig. 5) and the rate constants, equilibrium constants, and fluorescence levels given in Table 1.

used in purification. However, all of these explanations were either excluded or deemed to be very unlikely. In our earlier study (10) we also considered a version of the mechanism shown in Fig. 6 in which the conformational transitions were considered to be irreversible, i.e., proceeding only from E2 to E1. However, this model was unable to reproduce all of the observed experimental behavior. Using the fully reversible model shown in Fig. 6, both the time course (see Fig. 4) and the amplitudes (see Fig. 5) of the experimentally observed traces for the pig kidney enzyme can be adequately reproduced. The values of the rate constants, equilibrium constants, and fluorescence parameters used for the simulations are given in Table 1. All of the mathematical details of the simulations (i.e., the differential rate equations, calculation of the initial concentrations of the E2 and E2ATP states, and calculation of the total fluorescence) were previously described by Clarke et al. (10). Variations in the values of the parameters used for the simulations may yield some further improvement in the agreement between the simulations and the experimentally observed behavior. However, the set of parameter values used for the simulations shown in Figs. 4 *B* and 5 were based as far as possible on independent experimental measurements (see Table 1 and its footnotes for details). Using these parameters, the model captures all of the experimental observations, i.e., it quantitatively reproduces the ATP concentration dependence of the amplitudes (see Fig. 5), it reproduces the ATP-induced acceleration of the overall kinetics of the E2 $\rightarrow$ E1 transition, and, most importantly, it predicts the gradual conversion from biphasic to monophasic kinetics in the ATP concentration range of 0–50 μM.

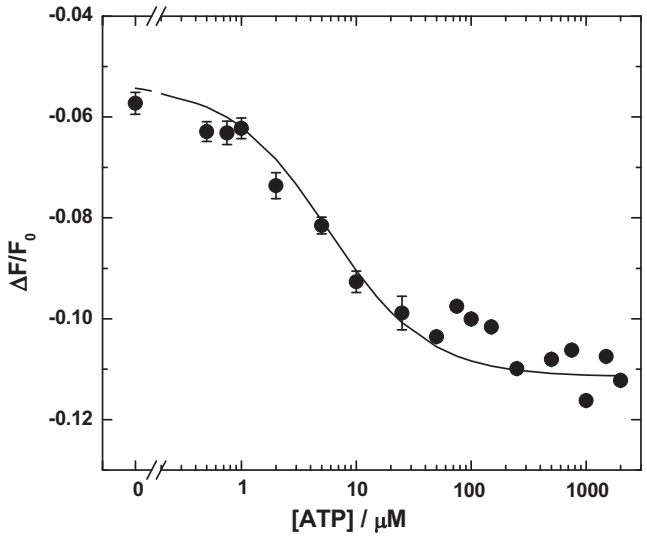

FIGURE 5 Amplitudes ($\Delta F/F_0$) of the fluorescence change observed in stopped-flow measurements on pig kidney Na^+,K^+-ATPase under the conditions described in Fig. 3 as a function of the ATP concentration. ΔF is the total fluorescence change (i.e., of both phases if a two-phase signal was observed), and F_0 is the initial fluorescence level before mixing with NaCl and ATP. The solid line represents the prediction of simulations based on a reversible dimeric conformational model (see Fig. 6). The values of $\Delta F/F_0$ were all determined from extrapolations to infinite time of either single or double exponential fits (whichever were more appropriate on the basis of residual plots) to the kinetic data.

DISCUSSION

The stopped-flow experiments described here revealed major differences in the kinetics and the mechanism of the E2 → E1 transition of the Na^+,K^+-ATPase from mammalian kidney and shark rectal gland. It is already widely known that ATP acts allosterically to accelerate the E2 → E1 conformational transition of unphosphorylated enzyme. However, the two enzyme preparations yield very different rate constants of the transition at saturating ATP concentrations. In the case of shark rectal gland, the experiments described here show that it reaches a value of 182 s^{-1}, whereas for enzyme from pig kidney the maximum value is only 38 s^{-1}. These values indicate that although the E2 → E1 transition is a major rate-determining step for the reaction cycle of the Na^+,K^+-ATPase from mammalian kidney, this is not the case for enzyme from shark rectal gland. Independent measurements (13,14) indicate that for this enzyme, the major rate-determining step is the K^+-stimulated dephosphorylation.

Another very significant difference between the kinetics of the E2 → E1 transition of mammalian enzyme and shark rectal gland is that for the mammalian enzyme it occurs as a two-step process in the absence of ATP, whereas for the shark enzyme it is a one-step process. This observation can be accounted for by the fact that the mammalian enzyme exists in the membrane in a diprotomeric form, $(\alpha\beta)_2$, whereas the shark enzyme exists in monoprotomeric form, $\alpha\beta$. In the absence of ATP, therefore, the transition of the mammalian enzyme is considered to occur via two consecutive steps, with three Na^+ ions binding immediately after each step, i.e., E2:E2 → E2:E1$(Na^+)_3$ → E1$(Na^+)_3$:E1$(Na^+)_3$. An analysis of the rates and amplitudes of the observed transients for pig kidney enzyme indicates that the first step occurs with a forward rate constant of ~13 s^{-1} and the second step occurs with a rate constant of ~0.5 s^{-1}. The slower rate of the second step can be explained by steric inhibition due to interactions between the neighboring α-subunits within the $(\alpha\beta)_2$ diprotomer. Crystallographic data on the related enzyme, the sarcoplasmic reticulum Ca^{2+}-ATPase (7,8), support this explanation, because it has been found that in the absence of bound ATP, the cytoplasmic domains of the E1 state of the enzyme are relatively widely spread.

As the ATP concentration was increased, the kinetics of the E2 → E1 transition of the pig kidney enzyme accelerated and became increasingly monophasic. This suggests that the enzyme converts to a monoprotomeric $\alpha\beta$ state after ATP binding. This is also in agreement with crystallographic data on the sarcoplasmic reticulum Ca^{2+}-ATPase (7,8), which show that binding of ATP to the E1 state causes its cytoplasmic domains to close up and adopt a much more compact conformation. Because these enzymes are packed to a very high density in their native membranes, this would be expected to decrease the extent of protein-protein interactions and allow the α-subunits to act independently, unaffected by the conformational state of a neighboring α-subunit within the membrane. This would explain the observed increasingly monophasic kinetics of the E2 → E1 transition as the ATP concentration increased. In this mechanism, therefore, the allosteric acceleration of the E2 → E1

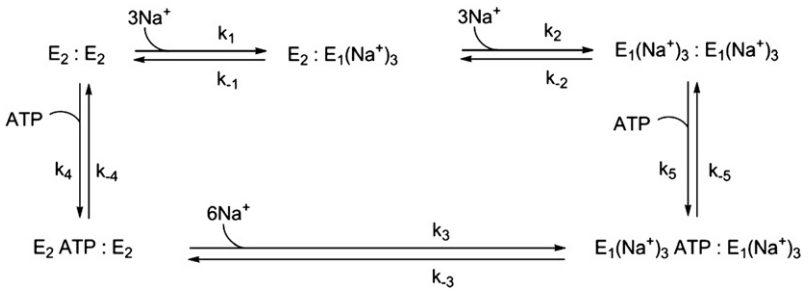

FIGURE 6 Reversible dimeric model of the E2 → E1 conformational change of pig kidney Na^+,K^+-ATPase.

TABLE 1 Values of the rate constants, equilibrium constants, and fluorescence parameters of the reversible dimeric conformational change model used for the simulations shown in Figs. 4 *B* and 5.

Parameter	Value	Reference
k_1	12.52 s^{-1}	This work*
k_{-1}	12.52 s^{-1}	This work*
k_2	0.4712 s^{-1}	This work†
k_{-2}	0.4712 s^{-1}	This work†
k_3	37.5 s^{-1}	This work‡
k_{-3}	0.5 s^{-1}	This work‡
k_4	52 μM^{-1} s^{-1}	This work§
k_{-4}	7436 s^{-1}	This work¶
k_5	52 μM^{-1} s^{-1}	This work§
k_{-5}	13 s^{-1}	(31)
K_A (= k_{-4}/k_4)	143 μM	(10)
K_A' (= k_{-5}/k_5)	0.25 μM	(32,33)
f_{E2}	1.0	This work‖
$f_{E2:E1}$	0.95	This work**
f_{E1}	0.887	This work***

*This value was chosen to closely reproduce the observed experimental ATP dependence of the time course and amplitudes of the fluorescence transients, and to satisfy the condition $(k_1 + k_{-1}) = 25.04$ s^{-1}, the experimentally determined observed rate constant of the fast phase observed in the absence of ATP.

†This value was chosen to closely reproduce the observed experimental ATP dependence of the time course and amplitudes of the fluorescence transients, and to satisfy the condition $(k_2 + k_{-2}) = 0.9424$ s^{-1}, the experimentally determined observed rate constant of the slow phase observed in the absence of ATP.

‡This value was chosen to closely reproduce the observed experimental ATP dependence of the time course and amplitudes of the fluorescence transients, and to satisfy the condition $(k_3 + k_{-3}) = 37$ s^{-1}, the experimentally determined observed rate constant of the fluorescence transient observed in the presence of ATP.

§The rate constants for ATP binding to the E2 state were taken to be equal to that of binding to the E1 state. The differences in their ATP affinities were assumed to be due to different dissociation rate constants alone. This value was estimated by dividing the dissociation rate constant by the ATP dissociation constant, i.e., $k_5 = k_4 = k_{-5}/K_A'$.

¶This value was estimated by multiplying the ATP dissociation rate constant for the E1 state by the ratio of the ATP dissociation constants of the E2 and E1 states, i.e., $k_{-4} = k_{-5}(K_A/K_A')$.

‖f_{E2} is the fluorescence level of the E2:E2 and E2ATP:E2 states. It was arbitrarily defined as 1.0 as a reference point for the fluorescence changes.

**$f_{E2:E1}$ and f_{E1} are the fluorescence levels of the E2:E1$(Na^+)_3$ state and E1$(Na^+)_3$:E1$(Na^+)_3$ states, respectively. Their values were estimated on the basis of the relative amplitudes of the two phases in the absence of ATP (i.e., 35% fast phase and 65% slow phase) and by approximating the fluorescence change of saturating conversion into the E1 state by the amplitude ($\Delta F/F_0$) at high levels of ATP of ~−0.11.

transition by ATP can be attributed to the relief of a preexisting steric inhibition of the enzyme arising from protein-protein interactions within an $(\alpha\beta)_2$ diprotomer due to the ability of ATP to close the enzyme's cytoplasmic domains and separate the α-subunits from each other.

However, in the case of the shark rectal gland enzyme, the kinetics of the E2 → E1 transition were monophasic at all ATP concentrations, and an acceleration of the transition was still observed. Therefore, for this enzyme, the mechanism of ATP-induced acceleration of diprotomeric enzyme just described for the pig kidney enzyme cannot be operating. The monophasic kinetics indicates that the enzyme is always monoprotomeric, $(\alpha\beta)$. Therefore, one must conclude that ATP has a separate mechanism whereby it can also accelerate the E2 → E1 transition of a single monoprotomer. In agreement with this result, Shinoda et al. (34) recently speculated, based on crystallographic studies, that the ATP-induced acceleration of the E2 → E1 transition of the shark rectal gland enzyme could be explained by the disruption of the salt bridge Glu^{223}-Arg^{551} by ATP binding. Because this salt bridge is the only connection between the A- and N-domains, ATP could then aid in the dissociation of the two domains from each other.

The differences in the oligomeric state of the mammalian kidney and the shark rectal gland enzymes raise the interesting question of what function protein oligomerization might have. Mammals, such as pigs and rabbits, are ectotherms (i.e., warm-blooded), whereas sharks are endotherms (i.e., cold-blooded). Their Na^+,K^+-ATPases have evolved to function at very different temperatures, i.e., ~8°C for shark and 37°C for pig and rabbit (35). Therefore, the shark enzyme does not need to have a high thermal stability. Comparative measurements of the inactivation of Na^+,K^+-ATPase activity from pig and shark have indeed shown that the shark enzyme has a much lower thermal stability, and differential scanning calorimetric measurements have shown that it denatures at a temperature ~10°C lower than that of pig enzyme (i.e., 45°C for shark versus 55°C for pig (35)). Therefore, a possible physiological function of oligomerization to an $(\alpha\beta)_2$ diprotomer in pig and rabbit kidney could be to enhance thermal stability at the higher body temperature of these animals relative to the shark. Previous studies have tended to attribute the higher thermal stability of mammalian enzymes to differences in their lipid environment and their association with small FXYD proteins (i.e., the γ-subunit in the case of mammalian kidney enzymes) (35–37). Nevertheless, if interaction with FYXD proteins increases thermal stability, it would seem logical that interaction between α-subunits within an $(\alpha\beta)_2$ diprotomer would enhance thermal stability even more. In fact, protein oligomerization is a well-documented strategy of proteins to increase thermal stability (38), and dimerization has been reported for many enzymes belonging to the P-type ATPase family, including prokaryotic members such as the K^+-translocating Kdp-ATPase from *Escherichia coli* (39). However, it is important to keep in mind that the experiments carried out here show that the $(\alpha\beta)_2$ diprotomer of the mammalian kidney enzymes is most stable when ATP is not bound, and that it is destabilized by interaction with ATP. Under normal physiological conditions of 1–5 mM ATP (40), the mammalian kidney enzymes would be expected, like the shark enzyme, to exist as $\alpha\beta$ monoprotomers. Therefore, protein oligomerization within mammalian kidney membranes may be a method of storing Na^+,K^+-ATPase in a less active but more highly thermal stable state

ready for stimulation and conversion into monoprotomers once the enzymes are supplied with a sufficiently high concentration of ATP. A further possible physiological role of dimer formation, which we postulated in previous studies (1,41,42), would be to enhance the enzyme's ATP binding affinity. This could allow the enzyme to continue to cycle, although at a low rate, under extreme hypoxic or anoxic conditions when the ATP level in the cell falls to a very low level, e.g., in the case of very low oxygen supply or extreme physical activity.

A final interesting question is whether dimer formation by the Na^+,K^+-ATPase is specific, i.e., whether it comes about via specific interactions between two α-subunits or occurs automatically due to a high protein density within the membrane. Analyses of purified native Na^+,K^+-ATPase membranes from shark rectal gland and pig kidney via electron microscopy have shown that the two preparations exhibit no significant difference in the frequency of intramembrane protein particles (43). This being the case, it would seem likely that dimer formation by the Na^+,K^+-ATPase in pig kidney membranes is due to specific protein-protein interactions.

The authors thank Prof. Helge Rasmussen, Royal North Shore Hospital, Sydney, for financial assistance supporting enzyme transport, and Dr. Toby Hudson for help with the statistical analysis.

R.J.C. received financial support from the Australian Research Council/National Health and Medical Research Council funded Research Network "Fluorescence Applications in Biotechnology and Life Sciences" (RN0460002).

REFERENCES

1. Clarke, R. J. 2009. Mechanism of allosteric effects of ATP on the kinetics of P-type ATPases. *Eur. Biophys. J.* 39:3–17.
2. Scheiner-Bobis, G. 2002. The sodium pump. Its molecular properties and mechanics of ion transport. *Eur. J. Biochem.* 168:123–131.
3. Lüpfert, C., E. Grell, …, R. J. Clarke. 2001. Rate limitation of the Na^+,K^+-ATPase pump cycle. *Biophys. J.* 81:2069–2081.
4. Steinberg, M., and S. J. D. Karlish. 1989. Studies on conformational changes in Na,K-ATPase labeled with 5-iodoacetamidofluorescein. *J. Biol. Chem.* 264:2726–2734.
5. Humphrey, P. A., C. Lüpfert, …, R. J. Clarke. 2002. Mechanism of the rate-determining step of the Na^+,K^+-ATPase pump cycle. *Biochemistry.* 41:9496–9507.
6. Kong, B. Y., and R. J. Clarke. 2004. Identification of potential regulatory sites of the Na^+,K^+-ATPase by kinetic analysis. *Biochemistry.* 43:2241–2250.
7. Sørensen, T. L.-M., J. V. Møller, and P. Nissen. 2004. Phosphoryl transfer and calcium ion occlusion in the calcium pump. *Science.* 304: 1672–1675.
8. Jensen, A.-M. L., T. L.-M. Sørensen, …, P. Nissen. 2006. Modulatory and catalytic modes of ATP binding by the calcium pump. *EMBO J.* 25:2305–2314.
9. Ward, D. G., and J. D. Cavieres. 1993. Solubilized α β Na,K-ATPase remains protomeric during turnover yet shows apparent negative cooperativity toward ATP. *Proc. Natl. Acad. Sci. USA.* 90:5332–5336.
10. Clarke, R. J., H.-J. Apell, and B. Y. Kong. 2007. Allosteric effect of ATP on Na^+,K^+-ATPase conformational kinetics. *Biochemistry.* 46:7034–7044.
11. Kane, D. J., K. Fendler, …, R. J. Clarke. 1997. Stopped-flow kinetic investigations of conformational changes of pig kidney Na^+,K^+-ATPase. *Biochemistry.* 36:13406–13420.
12. Clarke, R. J., D. J. Kane, …, E. Bamberg. 1998. Kinetics of Na^+-dependent conformational changes of rabbit kidney Na^+,K^+-ATPase. *Biophys. J.* 75:1340–1353.
13. Cornelius, F., N. Turner, and H. R. Z. Christensen. 2003. Modulation of Na,K-ATPase by phospholipids and cholesterol. II. Steady-state and presteady-state kinetics. *Biochemistry.* 42:8541–8549.
14. Cornelius, F. 1995. Phosphorylation/dephosphorylation of reconstituted shark Na^+,K^+-ATPase: one phosphorylation site per $\alpha\beta$ protomer. *Biochim. Biophys. Acta.* 1235:197–204.
15. Skou, J. C., and M. Esmann. 1988. Preparation of membrane Na^+,K^+-ATPase from rectal glands of *Squalus acanthias*. *Methods Enzymol.* 156:43–46.
16. Klodos, I., M. Esmann, and R. L. Post. 2002. Large-scale preparation of sodium-potassium ATPase from kidney outer medulla. *Kidney Int.* 62:2097–2100.
17. Ottolenghi, P. 1975. The reversible delipidation of a solubilized sodium-plus-potassium ion-dependent adenosine triphosphatase from the salt gland of the spiny dogfish. *Biochem. J.* 151:61–66.
18. Peterson, G. L. 1977. A simplification of the protein assay method of Lowry et al. which is more generally applicable. *Anal. Biochem.* 83:346–356.
19. Lowry, O. H., N. J. Rosebrough, …, R. J. Randall. 1951. Protein measurement with the Folin phenol reagent. *J. Biol. Chem.* 193: 265–275.
20. Jørgensen, P. L., and J. P. Andersen. 1988. Structural basis for E_1-E_2 conformational transitions in Na,K-pump and Ca-pump proteins. *J. Membr. Biol.* 103:95–120.
21. Karlish, S. J. D. 1980. Characterization of conformational changes in (Na,K) ATPase labeled with fluorescein at the active site. *J. Bioenerg. Biomembr.* 12:111–136.
22. Skou, J. C., and M. Esmann. 1983. The effects of Na^+ and K^+ on the conformational transitions of $(Na^+ + K^+)$-ATPase. *Biochim. Biophys. Acta.* 746:101–113.
23. Schuurmans Stekhoven, F. M. A. H., H. G. P. Swarts, …, S. L. Bonting. 1985. Na^+-like effect of imidazole on the phosphorylation of $(Na^+ + K^+)$-ATPase. *Biochim. Biophys. Acta.* 815:16–24.
24. Schuurmans Stekhoven, F. M. A. H., H. G. P. Swarts, …, J. J. De Pont. 1988. Phosphorylation of $(Na^+ + K^+)$-ATPase; stimulation and inhibition by substituted and unsubstituted amines. *Biochim. Biophys. Acta.* 937:161–176.
25. Mezele, M., E. Lewitzki, …, E. Grell. 1988. Cation selectivity of membrane proteins. *Ber. Bunsen-Ges.* 92:998–1004.
26. Grell, E., R. Warmuth, …, H. Ruf. 1991. Precision titrations to determine affinity and stoichiometry of alkali, alkaline earth, and buffer cation binding to Na,K-ATPase. *In* The Sodium Pump: Recent Developments. J. H. Kaplan and P. De Weer, editors. Rockefeller University Press, New York. 441–445.
27. Grell, E., E. Lewitzki, …, M. Doludda. 1994. Reassignment of cation-induced population of main conformational states of FITC-Na^+/K^+-ATPase as detected by fluorescence spectroscopy and characterized by equilibrium binding studies. *In* The Sodium Pump: Structure Mechanism, Hormonal Control and Its Role in Disease. E. Bamberg and W. Schoner, editors. Steinkopff Verlag, Darmstadt, Germany. 617–620.
28. Doludda, M., E. Lewitzki, …, E. Grell. 1994. Kinetics and mechanism of cation binding to Na^+,K^+-ATPase. *In* The Sodium Pump: Structure Mechanism, Hormonal Control and Its Role in Disease. E. Bamberg and W. Schoner, editors. Steinkopff Verlag, Darmstadt, Germany. 629–632.
29. Schneeberger, A., and H.-J. Apell. 2001. Ion selectivity of the cytoplasmic binding sites of the Na,K-ATPase: II. Competition of various cations. *J. Membr. Biol.* 179:263–273.
30. Apell, H.-J., and A. Diller. 2002. Do H^+ ions obscure electrogenic Na^+ and K^+ binding in the E1 state of the Na,K-ATPase? *FEBS Lett.* 532:198–202.

31. Fedosova, N. U., P. Champeil, and M. Esmann. 2002. Nucleotide binding to Na,K-ATPase: the role of electrostatic interactions. *Biochemistry*. 41:1267–1273.

32. Montes, M. R., R. M. González-Lebrero, …, R. C. Rossi. 2004. Quantitative analysis of the interaction between the fluorescent probe eosin and the Na^+/K^+-ATPase studied through Rb^+ occlusion. *Biochemistry*. 43:2062–2069.

33. Fedosova, N. U., P. Champeil, and M. Esmann. 2003. Rapid filtration analysis of nucleotide binding to Na,K-ATPase. *Biochemistry*. 42:3536–3543.

34. Shinoda, T., H. Ogawa, …, C. Toyoshima. 2009. Crystal structure of the sodium-potassium pump at 2.4 A resolution. *Nature*. 459: 446–450.

35. Fodor, E., N. U. Fedosova, …, M. Esmann. 2008. Stabilization of Na,K-ATPase by ionic interactions. *Biochim. Biophys. Acta*. 1778: 835–843.

36. Haviv, H., E. Cohen, …, S. J. Karlish. 2007. Stabilization of Na^+,K^+-ATPase purified from *Pichia pastoris* membranes by specific interactions with lipids. *Biochemistry*. 46:12855–12867.

37. Lifshitz, Y., E. Petrovich, …, S. J. Karlish. 2007. Purification of the human $\alpha 2$ isoform of Na,K-ATPase expressed in *Pichia pastoris*. Stabilization by lipids and FXYD1. *Biochemistry*. 46:14937–14950.

38. Rees, D. C. 2001. Crystallographic analyses of hyperthermophilic proteins. *Methods Enzymol*. 334:423–437.

39. Heitkamp, T., R. Kalinowski, …, J. C. Greie. 2008. K^+-Translocating KdpFABC P-type ATPase from *Escherichia coli* acts as a functional and structural dimer. *Biochemistry*. 47:3564–3575.

40. Gribble, F. M., G. Loussouarn, …, F. M. Ashcroft. 2000. A novel method for measurement of submembrane ATP concentration. *J. Biol. Chem*. 39:30046–30049.

41. Clarke, R. J., and D. J. Kane. 2007. Two gears of pumping by the sodium pump. *Biophys. J*. 93:4187–4196.

42. Pilotelle-Bunner, A., J. M. Matthews, …, R. J. Clarke. 2008. ATP binding equilibria of the Na^+,K^+-ATPase. *Biochemistry*. 47:13103–13114.

43. Ning, G., A. B. Maunsbach, and M. Esmann. 1993. Ultrastructure of membrane-bound Na, K-ATPase after extensive tryptic digestion. *FEBS Lett*. 330:19–22.